2018 25th International Lightning Detection Conference &
7th International Lightning Meteorology Conference
March 12 - 15 | Ft. Lauderdale, Florida, USA

ENSO Related Interannual Lightning Variability from the Full TRMM LIS Lightning Climatology

Austin Clark
Dept. of Atmospheric Science
University of Alabama in Huntsville
Huntsville, AL, USA
ac0028@uah.edu

Daniel Cecil
NASA Marshall Space Flight Center
Huntsville, AL, USA
daniel.j.cecil@nasa.gov

***Abstract*— It has been shown that the El Niño/Southern Oscillation (ENSO) contributes to inter-annual variability of lightning production in the tropics and subtropics more than any other atmospheric oscillation. This study further investigated how ENSO phase affects lightning production in the tropics and subtropics. Using the Tropical Rainfall Measuring Mission (TRMM) Lightning Imaging Sensor (LIS) and the Oceanic Niño Index (ONI) for ENSO phase, lightning data were averaged into corresponding mean annual warm, cold, and neutral 'years' for analysis of the different phases. An examination of the regional sensitivities and preliminary analysis of three locations was conducted using model reanalysis data to determine the leading convective mechanisms in these areas and how they might respond to the ENSO phases. These processes were then studied for inter-annual variance and subsequent correlation to ENSO during the study period to best describe the observed lightning deviations from year to year at each location.**

Keywords—Lightning; ENSO; Climatology; LIS

I. INTRODUCTION

The El Niño/Southern Oscillation (ENSO) has been widely studied with respect to how it can affect global atmospheric patterns [e.g Ropelewski and Halpert, 1986, 1987; Latif et al., 1998; Wright et al., 1998; Dai and Wigley, 2000]. As a result, it has been shown that ENSO is the largest inter-annual contributor to atmospheric variability in the tropics and subtropics. This variability is strongly dependent on phase and geographic location, with phase magnitude playing a less understood role [Sátori et al., 2009]. It would be expected then that ENSO would also play a significant role in the variability of lightning around the globe, however until recently this had been relatively uninvestigated on the global or climatological scales. The launch of the Optical Transient Detector (OTD) in 1995 and subsequent launch of the Tropical Rainfall Measuring Mission (TRMM) Lightning Imaging Sensor (LIS) in 1998 made these investigations possible, especially given the extended operation of LIS [Boccippio et al., 2002]. These space-based observations provide one of the most spatiotemporally continuous climatological lightning datasets currently available. With near-global lightning data becoming readily and reliably available for study in the past 25 years, several studies were conducted of lightning production during individual ENSO events and at ENSO time scales using satellite observations and/or very low frequency (VLF) long range ground networks [e.g. Goodman et al., 2000; Hamid et al., 2001; Chronis et al., 2008; LaJoie and Laing, 2008; Laing et al., 2008; Sátori et al., 2009; Collier and Hughes, 2011; Bovalo et al., 2012; Dowdy, 2016]. These studies have identified global responses to ENSO phase as well as individual areas that show different responses to ENSO phase. These locations include but are not limited to the Northern Coast of the Gulf of Mexico, the Maritime Continent, Northern Australia, the Equatorial Atlantic and Pacific, Southeast Asia, India, Argentina and Brazil. This study looked to build upon the previous work, expanding the number of ENSO cases and utilizing the full climatology of LIS to further study the impacts of ENSO on tropical and sub-tropical lightning production as well as the mechanisms causing the variability.

II. DATA AND METHODS

A. Lightning Data

The primary dataset used for the analysis of lightning variability is the LIS Low Resolution Time Series (LRTS) from the Gridded Lightning Climatology from TRMM LIS and OTD [Cecil et al., 2014]. LIS collected data from January of 1998 until May of 2015, covering to 38° north and south on a 35° inclination low Earth orbit. LIS had a diurnal average 82% detection efficiency with near uniform geographic detection efficiency and average 5km spatial resolution in a 600×600 km swath [Cecil et al., 2014]. More details about the LIS instrument were described by Boccippio et al. [2002]. The LIS LRTS is at

NASA Weather and Atmospheric Dynamics Program (NNH16ZDA001)

2.5°×2.5° spatial resolution and is smoothed spatially by 7.5° and temporally by 99 days using a moving boxcar average. A low pass digital filter was then applied after the initial smoothing. This allows for a smooth and continuous time series to be constructed averaging over the diurnal patterns for each location, but as a result the exact flash rate on any given day is essentially a seasonal average. This heavy smoothing also allowed for the long-term trends to show more prominently and helped to minimize shorter term variability, such as very large events, while still allowing seasonal and annual variability. Additional information on the LRTS can be found within the Cecil et al. [2014] dataset description. These data were used to create averages based on ENSO phase as well as show the total time series for each selected location. Although OTD data is included in this dataset, everything presented here uses only LIS data. OTD had a much shorter operational period and detection efficiency when compared to LIS; however, it did cover the midlatitudes with a 70° inclination orbit and observed the record 1997/1998 El Niño and so future plans are to incorporate the OTD data and expand the number of ENSO episodes.

B. Model Data

The lightning data were compared to model data using the NCEP/NCAR 40 Year Reanalysis Project (hereinafter referred to as NCNC) [Kalnay et al., 1996]. The NCNC data used was comprised of both $2.5° \times 2.5°$ gridded and T62 spectral daily averages. The T62 data was slightly higher resolution than the gridded data and was resampled to a lower resolution to match the gridded NCNC data and LRTS. The NCNC data was then smoothed 7.5° and 99 days to maintain consistency with LRTS. The exceptions to this are CAPE and CIN, which used initially unsmoothed values for the computations and were later smoothed as standalone variables. Most of the variables used were surface based or atmospheric column values; however, temperature, height, and pressure data from all seventeen model levels were used to calculate CAPE and CIN respectively. Bolton [1980] approximations were used to determine the lowest condensation level (LCL) temperatures, heights, and pressures. If no LCL or level of free convection (LFC) was found for a given grid cell on any particular day, the values of both CAPE and CIN in that cell were set to zero, similar to Riemann-Campe et al., [2009]. Afterward, CAPE and CIN were calculated using interpolated integration methods between model levels from the model surface to the model tropospheric height in each grid cell. Daily averaged values as used here tend to underestimate magnitudes compared to the diurnal maximum when convection tends to form (e.g. CAPE over land), and as a result only the seasonal and annual trends are examined. Further study is planned to use the local daily maximum values to compare magnitudes of variables to the lightning magnitudes more directly.

C. ENSO Data

This study used what was coined an ENSO year, which effectively redefined a calendar year to encompass the peak of an ENSO phase within a single year. This was done by setting the beginning of the year as April 1st of the current year and then defining the end of the year as March 31st of the following year (e.g. ENSO 2000 would run from 4/1/2000 to 3/31/2001). This created an easy way to average ENSO phases together and create mean warm, cold, and neutral years. The years included began in April of 1998 and ended in March of 2014, giving sixteen ENSO years (1998-2013). In order to determine the sign of each ENSO year, the Oceanic Niño Index (ONI) was used [Huang et al., 2017]. The thresholds for the warm and cold years were a $0.5°\text{C}$ deviation from the thirty year mean for at least five consecutive three-month averages as described by Trenberth [1997]. Years that did not meet either of these thresholds were classified as neutral years. Overall, eight of the sixteen study years were classified as cold, leaving four as warm and four as neutral respectively. The individual years and their magnitudes are shown in Table 1. The average magnitude for the cold years was $-0.79°\text{C}$, the average warm magnitude was $+0.61°\text{C}$, and the average neutral magnitude was $-0.08°\text{C}$. Although there were several moderately strong La Niña events during the study period, only one such El Niño event was observed in 2009.

Once the classification of each individual year was completed, both the NCNC data and the LRTS were divided into warm, cold, and neutral years and binned into a 5°×5° grid for the entire LIS domain. LRTS for each individual year in every grid cell were plotted in reference to their phase against the mean annual pattern and the mean warm, cold, and neutral patterns. Visual analysis of these plots subjectively quantified the variance within the mean for each phase as well as the differences between the means at a given location. Given the limited number of warm and neutral years, individual outlier years sometimes significantly shifted the phase mean away from the patterns of the other phase years. Therefore, means biased towards outlier years were visually corrected towards the consensus of the other years of the same phase before assessing them as having a phase sensitivity. All of the individual plots were then projected onto the globe in their respective location using Google Earth to visualize the spatial variation in the phase patterns as well as their seasonality on an interactive platform. An example of this is in Fig. 1 for Southeastern Africa and Madagascar. Adjacent plots with similar annual patterns and phase sensitivities were then averaged together, in 10°×15° areas. To be considered in the study, the overall mean lightning production in the averaged area had to be at least $3\text{Flkm}^{-2}\text{Yr}^{-1}$ to minimize the effect of smaller scale variations. This mostly served to filter out open ocean and desert regions where little lightning occurs, and variability between individual years could be greater than the mean annual flash rate. Ten of these locations were ultimately chosen, with priority given to phase dependence and geographic location in order to differentiate between phases and the direct impacts of ENSO versus teleconnections.

III. RESULTS

The results in this paper are split into two portions- the first describes the observations in the lightning data with respect to ENSO, and the second describes the variation of the environmental characteristics in three of these locations and how they may potentially relate to the observed lightning variability.

TABLE I. ONI VALUES FOR EACH THREE-MONTH AVERAGING PERIOD. COLORED VALUES INDICATE ONI THRESHOLD MET; COLORED SHADING INDICATES INCLUSION IN THE STUDY AS EITHER A WARM (RED), COLD (BLUE), OR NEUTRAL (GRAY) YEAR

Year	DJF	JFM	FMA	MAM	AMJ	MJJ	JJA	JAS	ASO	SON	OND	NDJ
1997	-0.5	-0.4	-0.1	0.3	0.8	1.2	1.6	1.9	2.1	2.3	2.4	2.4
1998	2.2	1.9	1.4	1	0.5	-0.1	-0.8	-1.1	-1.3	-1.4	-1.5	-1.6
1999	-1.5	-1.3	-1.1	-1	-1	-1	-1.1	-1.1	-1.2	-1.3	-1.5	-1.7
2000	-1.7	-1.4	-1.1	-0.8	-0.7	-0.6	-0.6	-0.5	-0.5	-0.6	-0.7	-0.7
2001	-0.7	-0.5	-0.4	-0.3	-0.3	-0.1	-0.1	-0.1	-0.2	-0.3	-0.3	-0.3
2002	-0.1	0	0.1	0.2	0.4	0.7	0.8	0.9	1	1.2	1.3	1.1
2003	0.9	0.6	0.4	0	-0.3	-0.2	0.1	0.2	0.3	0.3	0.4	0.4
2004	0.4	0.3	0.2	0.2	0.2	0.3	0.5	0.6	0.7	0.7	0.7	0.7
2005	0.6	0.6	0.4	0.4	0.3	0.1	-0.1	-0.1	-0.1	-0.3	-0.6	-0.8
2006	-0.8	-0.7	-0.5	-0.3	0	0	0.1	0.3	0.5	0.7	0.9	0.9
2007	0.7	0.3	0	-0.2	-0.3	-0.4	-0.5	-0.8	-1.1	-1.4	-1.5	-1.6
2008	-1.6	-1.4	-1.2	-0.9	-0.8	-0.5	-0.4	-0.3	-0.3	-0.4	-0.6	-0.7
2009	-0.8	-0.7	-0.5	-0.2	0.1	0.4	0.5	0.5	0.7	1	1.3	1.6
2010	1.5	1.3	0.9	0.4	-0.1	-0.6	-1	-1.4	-1.6	-1.7	-1.7	-1.6
2011	-1.4	-1.1	-0.8	-0.6	-0.5	-0.4	-0.5	-0.7	-0.9	-1.1	-1.1	-1
2012	-0.8	-0.6	-0.5	-0.4	-0.2	0.1	0.3	0.3	0.3	0.2	0	-0.2
2013	-0.4	-0.3	-0.2	-0.2	-0.3	-0.3	-0.4	-0.4	-0.3	-0.2	-0.2	-0.3
2014	-0.4	-0.4	-0.2	0.1	0.3	0.2	0.1	0	0.2	0.4	0.6	0.7

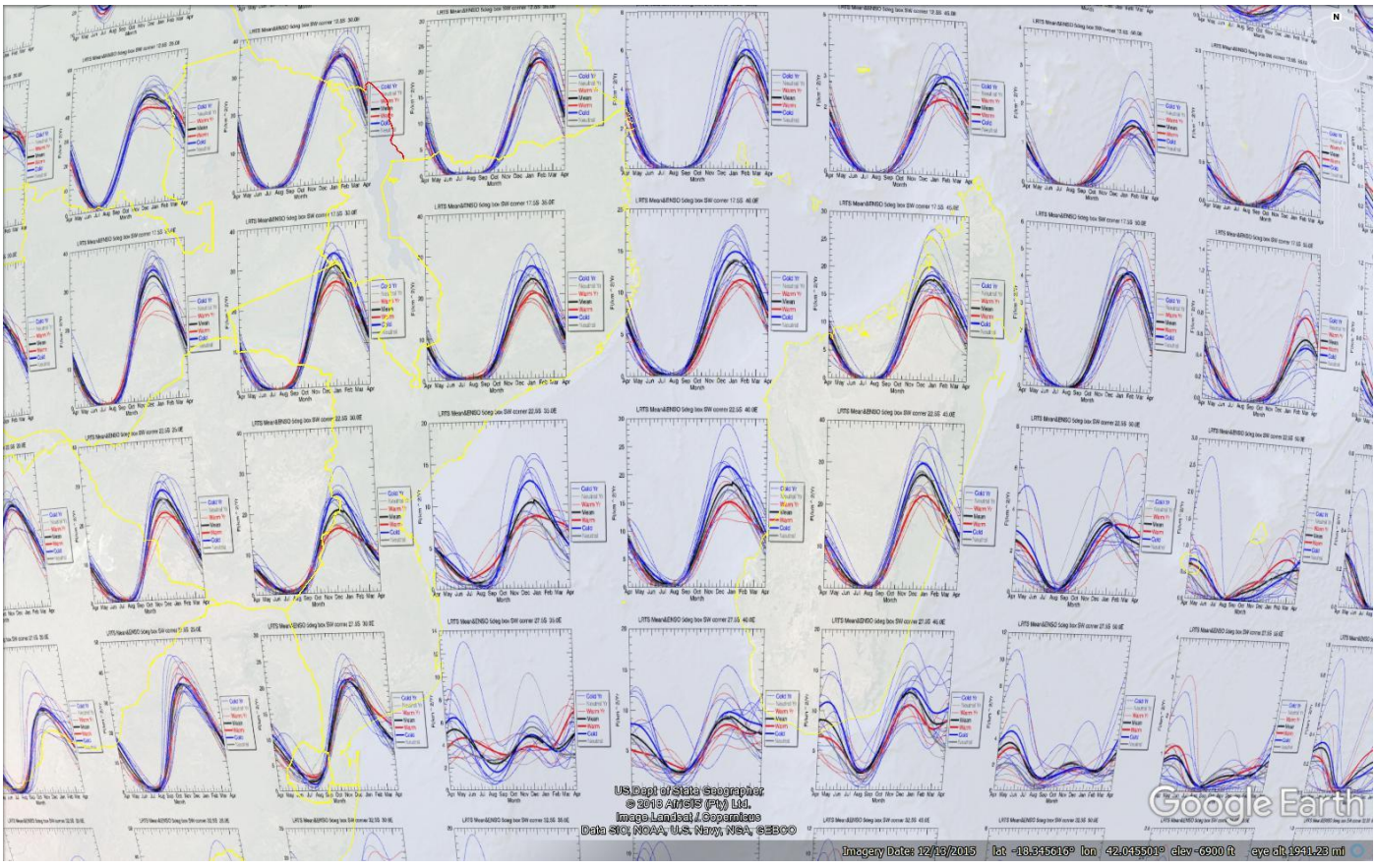

Fig. 1. Example Google Earth visualization of individual years and mean ENSO LRTS lightning data over an ENSO year for Mozambique, Madagascar, the Mozambique Channel, and southwestern Indian Ocean. Red is warm, blue is cold, gray is neutral, and black is the mean annual patter

A. *Regional Sensitivities*

This study identified several areas with potential connections to ENSO phase as well as some locations with significant annual variability and no clear connection to the phase of ENSO. Fig. 2 displays the overall deviation from the mean flash rate for the warm, cold, and neutral phases as well as the percent deviation compared to the mean flash rate. It should be noted that the plots only show total deviations for each phase and thus seasonal variations can have different signs or magnitudes for a location. The percentage maps appear quite noisy over the oceans due to most oceanic regions averaging less than $0.25\text{Flkm}^{-2}\text{Yr}^{-1}$ and as a result a single meteorological event can greatly affect the percentage deviations. These percentage maps suggest that ENSO can have a profound relative effect on oceanic lightning, especially in the Equatorial Pacific, Central Atlantic, and the Californian and Chilean coasts. The latter potentially suggesting a connection between the cold coastal currents that give California and Chile their unique climates and the weakening trade winds during El Niño. When compared to the magnitude maps, the maxima shift towards the land where significantly more lightning occurs.

Two warm phase maxima feature prominently, one in Central Africa and the other in subtropical South America. These regions both produce a significant amount of lightning in the annual cycle, with low resolution maxima near $50\text{Flkm}^{-2}\text{Yr}^{-1}$ in South America and $70\text{Flkm}^{-2}\text{Yr}^{-1}$ in Central Africa respectively. The Central Africa anomaly is on the northern fringes of the global lightning maxima in the Democratic Republic of the Congo. Both also have an increase in average annual lightning activity of over $6\text{Flkm}^{-2}\text{Yr}^{-1}$. Increases in lightning activity of slightly smaller magnitudes are also observed in eastern China, the Bay of Bengal, the Gulf of Mexico, the Middle East, and Malaysia. Significant negative anomalies during the warm phase are observed in Brazil, Australia, and Southeastern Africa. Three of the largest positive anomalies in the cold phase occur in Australia, Southeastern Africa, and Brazil in essentially the same areas and with the same magnitudes as the negative anomalies during the warm phase. Additionally, moderate positive anomalies are observed over western Africa and the equatorial Eastern Atlantic, the Eastern United States, and the Red Sea. Although the Central Africa region does seem to experience slightly less lightning during the cold phase, deviations of less than $1\text{Flkm}^{-2}\text{Yr}^{-1}$ are observed over a much smaller area which is likely insignificant when compared to the mean flash rate and the warm phase anomaly. In subtropical South America, a negative anomaly in the cold phase matching the size and intensity of the warm phase positive anomaly is observed. During the neutral pattern, the two lightning hotspots of Lake Maracaibo in Venezuela and the Democratic Republic of the Congo have positive anomalies. Other positive anomalies include Central South America, eastern Australia, the Arabian Peninsula, the Himalayas, and the Florida Peninsula down into Cuba. Convection in several of these locations is driven in large part by local processes such as sea breezes, differential heating, and topography; none of which are directly affected by ENSO phase and could be evidence for minimal impact from ENSO in those locations.

Overall, these anomalies were analyzed in addition to the annual patterns from the Google Earth visualization, and ten locations were chosen for further examination. Two direct connections were chosen with one for each phase; the cold being in Brazil and the warm in Argentina. These locations were chosen because of the clear dichotomy in the observed lightning production between the warm and cold phases, and because of their proximity to the Equatorial Pacific where ENSO would be expected to play a large role. Four teleconnections were identified, with two of each phase: Southeastern Africa and the Red Sea for the cold phase, and Central Africa and the Middle East for the warm phase. These locations displayed consistent sensitivity to a particular phase far from the more direct effects of ENSO and also have very different convective mechanisms, prompting questions as to why there would be ties to ENSO. Four null cases were also identified: Cuba and the Florida Peninsula, the Western South Atlantic and Uruguay, Myanmar and the Eastern Bay of Bengal, and the Maritime Continent centered on Singapore. The null locations were defined as areas where there was minimal inter-annual variability, significant variability with no correlation to ENSO phase, or where the null ENSO years have stronger magnitudes than the annual, warm, and cold means. Fig. 3 displays all ten locations over the low resolution mean annual flash rate.

B. *Closer Examinations*

A closer look into the lightning variability was conducted for the Central Africa, Southeastern Africa, and the Cuba/Florida Peninsula regions. The overall annual lightning patterns for each of these locations are in Fig. 4. The two African regions were chosen because during investigation it was found that they were linked by the same general process. The Cuban region was chosen because it incorporated the continental United States (CONUS) lightning maximum in Florida and two different convective mechanisms.

Convection in Africa is enhanced by the inter-tropical convergence zone (ITCZ) and its annual progression through the year. Collier and Hughes [2011] describe the general pattern of the ITCZ in Africa and how it is not a perfect descriptor of lightning activity across the continent but that the activity does follow the general pattern as the sun declination angle progresses. One key factor is the southward push of the ITCZ in eastern Africa, routinely making it to 15°S [Nassor and Jury, 1997]. As a first guess, it was hypothesized that observed lightning variability would likely be linked to changes in the ITCZ with ENSO phase for both African locations. A link to a large-scale process would also help explain the consistency with which the lightning production changed from one phase to another.

From previous literature, some changes in the ITCZ with ENSO were an enhancement in the speed of the southerly progression and the extent during cold phase years and a repressed southern extension during warm phase years [Nassor and Jury, 1997]. Additionally, it is noted that the descending

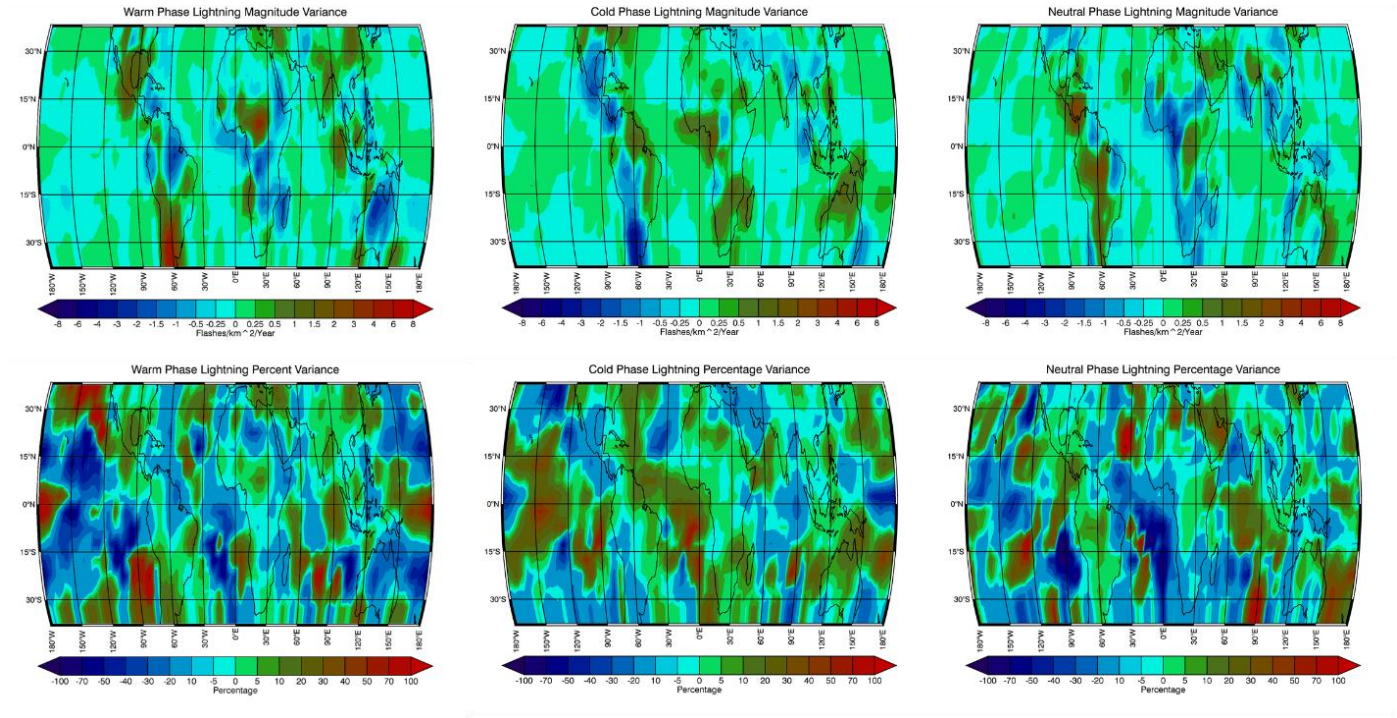

Fig. 2. Total deviation from the mean for the warm (left), cold (center), and neutral (right) phases in $\mathrm{Flkm^{-2}Yr^{-1}}$ (top) and percent of the mean annual flash rate for the cell (bottom).

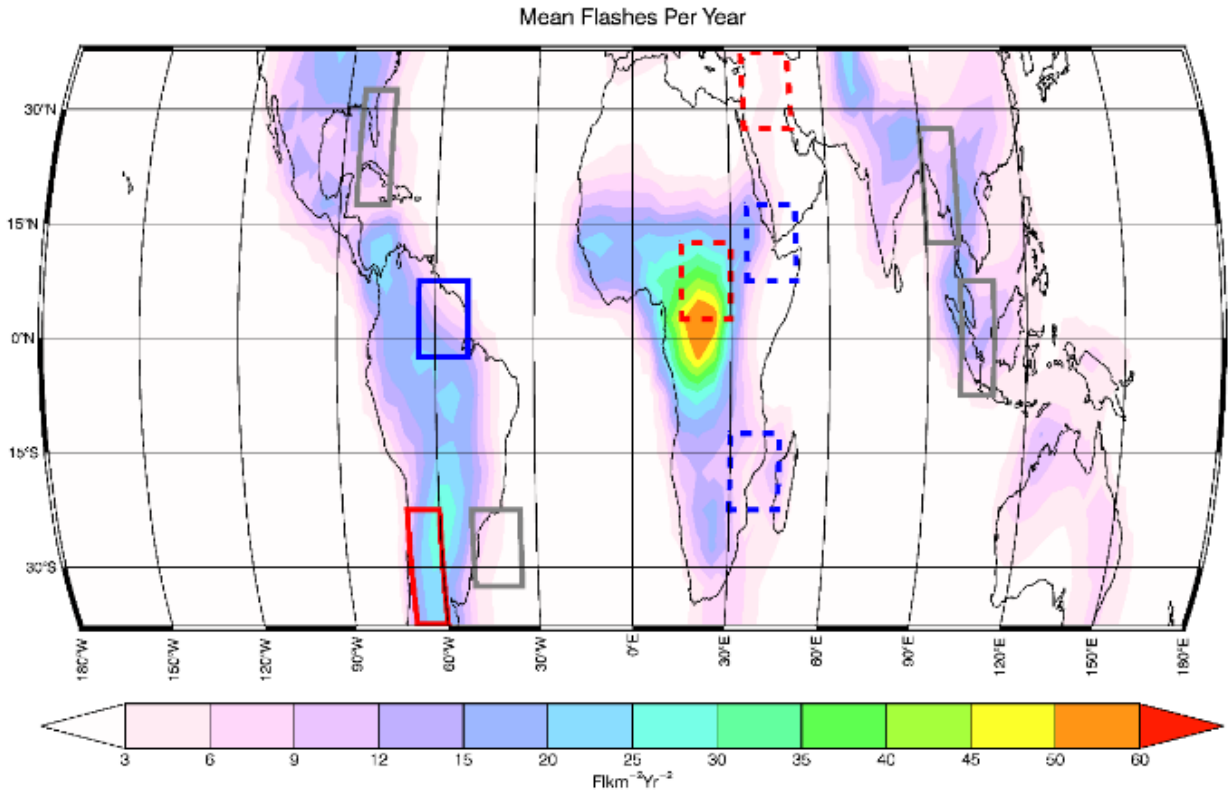

Fig. 3. Mean flash density (in $\mathrm{Flkm^{-2}Yr^{-1}}$) with overlaid study locations. Red boxes are warm, blue are cold, and gray are the null cases. For the warm and cold regions, solid boxes indicate direct connections and dashed boxes indicate teleconnections.

branch of the Hadley cell is stronger for El Niño years [Sátori et al., 2009]. Stronger subsidence in the upper levels can intensify the capping inversion by warming and drying the low levels. A stronger cap can intensify localized lightning activity by reducing the amount of widespread convection, conserving lower level moisture and energy for a few intense updrafts. These intense updrafts are able to loft more water vapor higher into the atmosphere, generating higher ice concentrations and resulting in more lightning.

1) Central Africa Region

In the Central Africa location, there is a distinct shift in the lightning maximum to later in the year during warm phase years, with an enhancement in lightning activity as well. Earlier in the year however there is little difference between any of the phases and some cold years show significant increases in lightning during the first peak in June but quickly fall back off. The El Niño years rather tend to keep increasing lightning production until August and then remain elevated until early October before realigning with the other means. In this way, the warm phase years effectively extend the maximum lightning production for an additional eight to ten weeks. There is also a northward extension of the lightning maximum, covering much of the designated region as illustrated in Fig. 5. These two shifts in the lightning activity could potentially be explained by the changes in the ITCZ. During the warm phase events, there is more southerly wind momentum during the austral summer near Madagascar. This in turn keeps the ITCZ from pushing as far south and allows for a longer residence time over the Central Africa regions, which could potentially explain the prolonged activity.

Also, recall that the capping inversion is stronger during the warm phase to the north of the ITCZ. This cap is a key component of convection in Central Africa, as much of the convection has an elevated base which means that the environment is generally capped [Christian et al., 2003]. Increasing its strength then could increase the strength of the convection that is able to penetrate out of the boundary layer. A slightly stronger capping inversion seems to be evidenced in Fig. 5 as well, with lower overall convective precipitation rates and a decrease in the extent of the precipitation maxima. This could explain the heightened lightning activity extending north of the ITCZ, where the correlation of surface moisture convergence and the enhanced subsidence is maximized [Sátori et al., 2009]. The extension of the lightning activity later into the year also means that it coincides with the maxima in moisture, CAPE, and LI respectively as evidenced by the correlations with NCNC data during the warm phase (Table 2). This could also help explain the enhancement in observed lightning activity.

2) Southeastern Africa Region

In Mozambique and Madagascar, there is a very clean separation between the warm, cold, and neutral phases, though the peak for each occurs about the same time. The La Niña lightning activity appears to be consistently elevated during the austral summer, whereas El Niño appears to suppress lightning activity and the neutral and mean patterns fall in the middle between the two. In Fig. 6, a larger extent of enhanced convective precipitation rate can be observed in the cold phase when compared to the mean patterns as well as a slight enhancement in northerly flow. The enhanced northerly flow forces the ITCZ further southward, increasing lightning activity further south into the Southeastern Africa box. The opposite is true during the warm phase, as there is an increase in southerly momentum which keeps the ITCZ further north and out of the region, decreasing lightning activity. NCNC data seems to support this, as stronger negative correlations are observed with the 10m meridional (V) wind during the cold phase (Table 3). There is also an expansion of the $30\text{Flkm}^{-2}\text{Yr}^{-1}$ region a local maximum of $35\text{Flkm}^{-2}\text{Yr}^{-1}$ over Madagascar during the cold phase which is not present in the mean pattern or warm phase.

3) Cuba and the Florida Peninsula

Convection in this region is not driven nearly as much by large scale lift or circulation but is more heavily influenced by local dynamic and thermodynamic processes. The lightning activity is peaked in the summer months and is primarily controlled by the sea breeze over Florida and the differential heating of the mountainous terrain in Cuba, as well as the orographic lift they provide. These processes are not heavily impacted by ENSO phase, as evidenced by the significant variability from year to year and even between years of the same phase in Fig. 4. Two years do stand out, the first being 2012 when the Southeastern US suffered a severe drought which effectively eliminated the Floridian lightning maximum [Koshak et al., 2015]. The second is early 2003, when there is an increase in lightning production during the severe weather season for the southeast. The correlations for Cuba against the NCNC data (Table 3) show that there is potentially a shift in large scale stability and lift between the warm and cold phases as a rather drastic shift in the annual pattern for omega. This change is displayed in Fig. 7. There could potentially be a 'net-zero' effect then, where the more stable warm phase produces fewer, stronger thunderstorms and the less stable cold phase produces more weak thunderstorms, and the two ultimately cancel, but this needs to be investigated further. There is a well-known tie to ENSO in Florida in regard to warm phase severe weather during the spring, potentially explaining the anomaly in 2003. It does not appear to play a significant role in inter-annual lightning variability however given that mesoscale convective systems (MCSs), as associated with the severe weather season, are not the major lightning producers for the region.

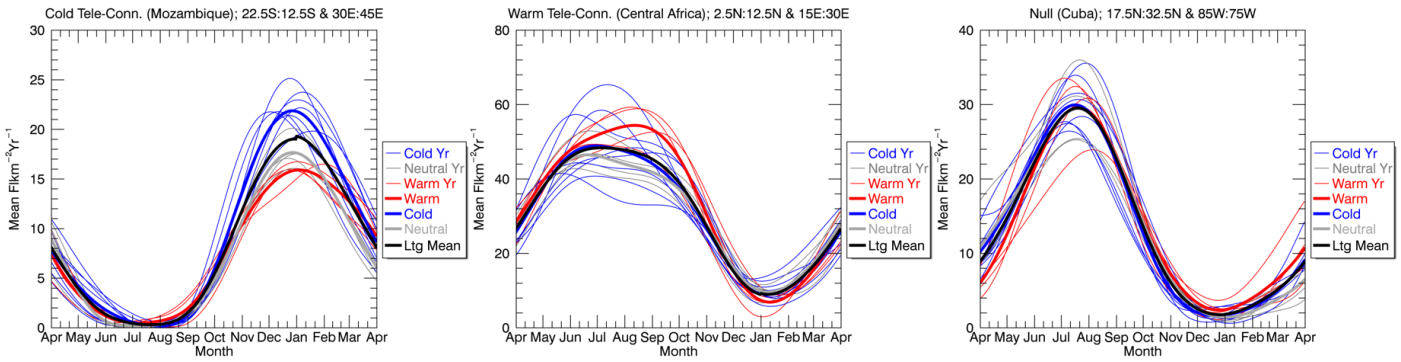

Fig. 4. ENSO Annual Patterns for the three study areas in (Flkm^{-2}Yr^{-1}) with the Southeastern Africa cold teleconnection (left), the Central Africa warm teleconnection (center), and the Cuban null case (right). Thin lines represent individual ENSO years, thick lines are the ohase means.

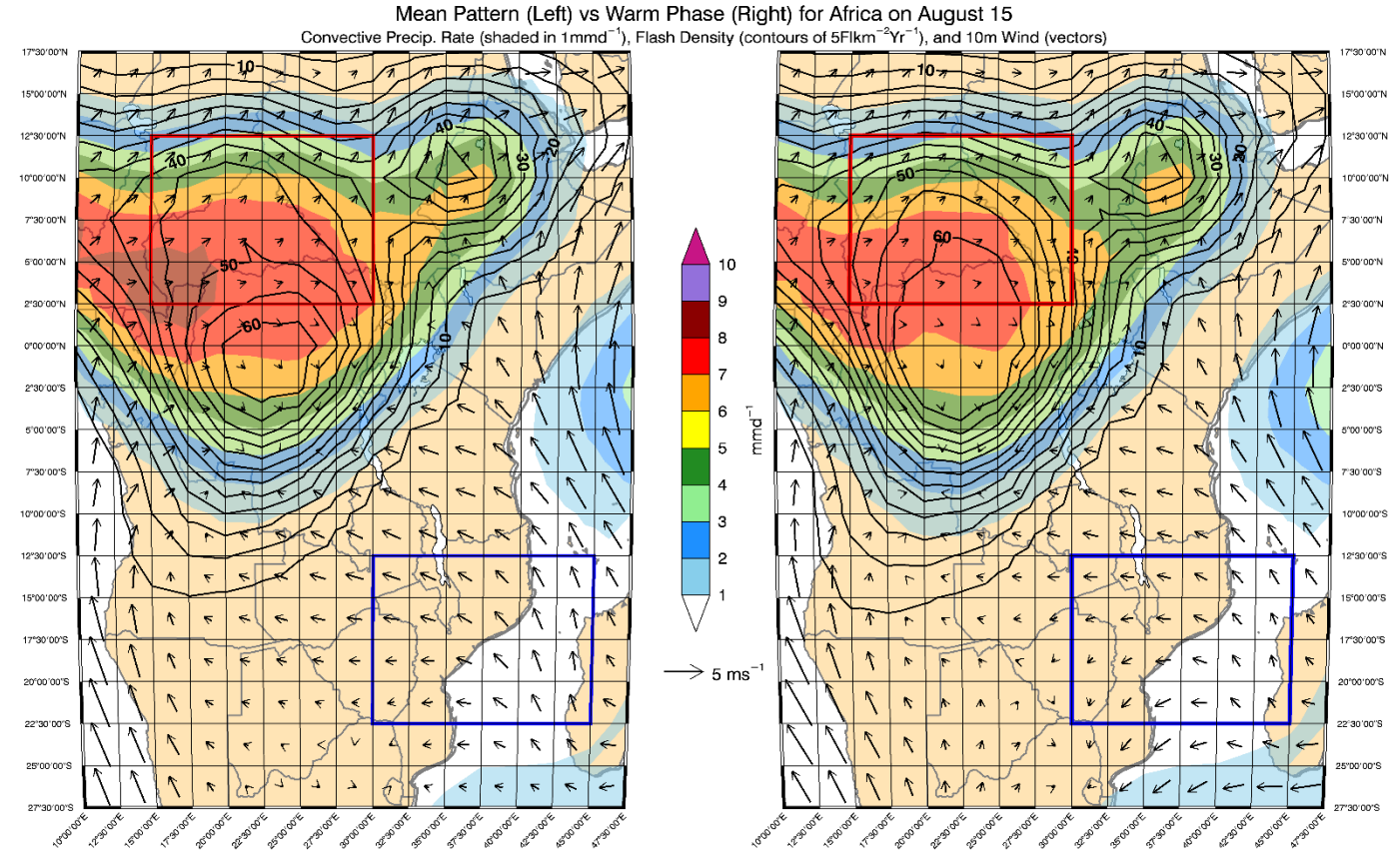

Fig. 5. LRTS (black contours, in Flkm^{-2}Yr^{-1}), NCNC convective precipitation (shaded contours in mmd^{-1}), and 10m wind (vectors in ms^{-1}) with the Central Africa (red box) and Southeastern Africa (blue box) identified. Mean pattern is on the left and the warm phase pattern is on the right for August 15th, during the warm phase lightning peak for the Central Africa region.

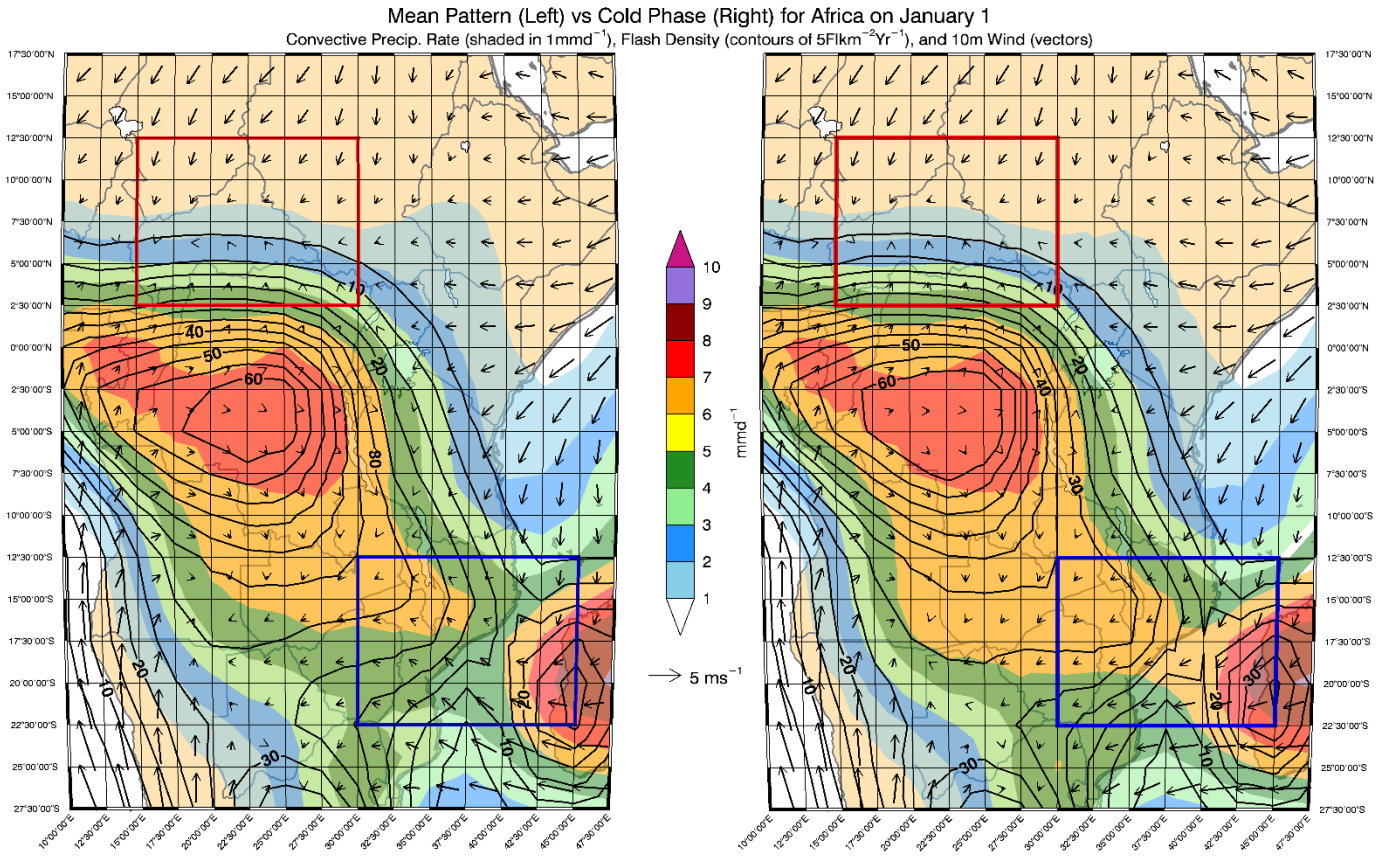

Fig. 6. As in Fig. 5, with the mean pattern on the left and cold phase pattern on the right for January 1st, during the cold phase lightning peak for the Southeastern Africa region.

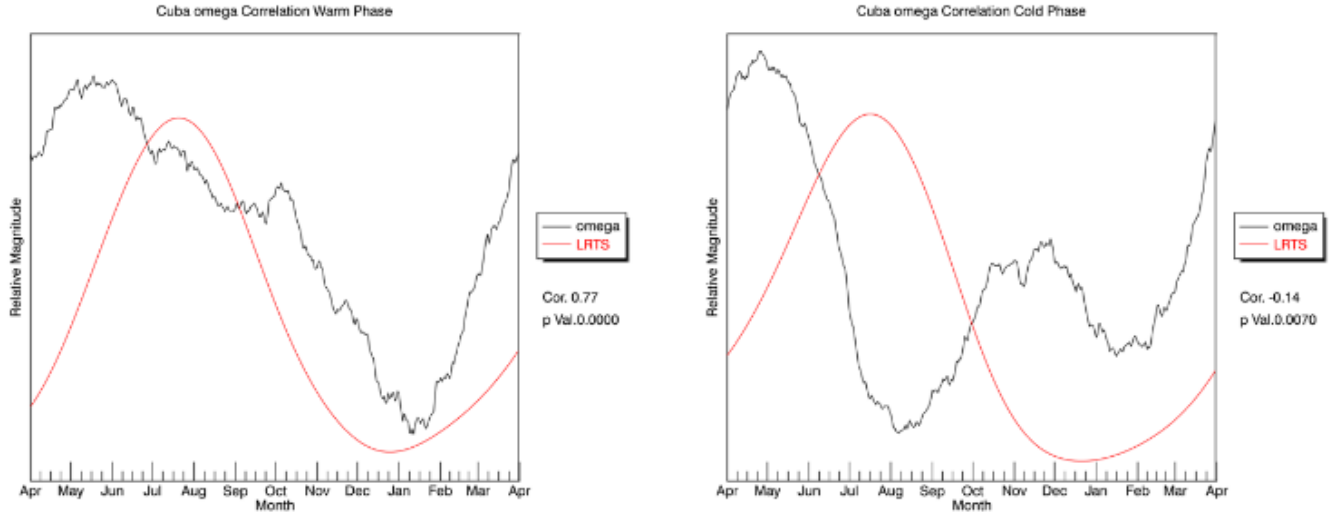

Fig. 7. Change in omega between the warm (left) and cold (right) phases with the relative annual trends for the NCNC omega (in black) and LRTS (in red).

TABLE II. CORRELATION VALUES FOR CENTRAL AFRICA OVER AN ENSO YEAR FOR EACH RESPECTIVE PHASE, AS WELL AS FROM JANUARY 1ST OF 1998 TO DECEMBER 31ST OF 2014

Variable	Annual	Warm	Cold	Neutral	Full
CAPE	0.894	0.938	0.883	0.869	0.778
Conv. Precip. Rate	0.846	0.891	0.839	0.811	0.707
LI	-0.949	-0.991	-0.940	-0.915	-0.891
Omega	-0.933	-0.935	-0.912	-0.901	-0.740
SFC Pressure	0.593	0.547	0.602	0.515	0.422
Precip. Water	0.955	0.991	0.948	0.924	0.881
SFC RH	0.822	0.883	0.811	0.785	0.783
SFC Temperature	-0.181	-0.201	-0.161	-0.133	-0.084
2m SHUM	0.868	0.930	0.858	0.833	0.825
10m U Wind	0.985	0.997	0.975	0.962	0.907
10m V Wind	0.978	0.908	0.989	0.986	0.907

[a.] Statistical significance at the 95% confidence interval was calculated to be $r > \sim|0.1|$ for the annual cycles and $r > \sim|0.025|$ for the full period

TABLE III. AS IN TABLE 2 FOR SOUTHEASTERN AFRICA

Variable	Annual	Warm	Cold	Neutral	Full
CAPE	0.945	0.951	0.937	0.936	0.923
Conv. Precip. Rate	0.871	0.905	0.869	0.845	0.785
LI	-0.955	-0.977	-0.944	-0.946	-0.939
Omega	-0.446	-0.315	0.047	-0.728	-0.190
SFC Pressure	-0.973	-0.976	-0.962	-0.974	-0.945
Precip. Water	0.933	0.961	0.924	0.917	0.907
SFC RH	0.589	0.656	0.601	0.524	0.593
SFC Temperature	0.912	0.927	0.907	0.912	0.863
2m SHUM	0.891	0.912	0.887	0.865	0.868
10m U Wind	0.381	0.403	0.366	0.325	0.341
10m V Wind	-0.931	-0.930	-0.962	-0.881	-0.890

TABLE IV. AS IN TABLE 2 FOR CUBA/FLORIDA PENINSULA

Variable	Annual	Warm	Cold	Neutral	Full
CAPE	0.943	0.937	0.933	0.946	0.908
Conv. Precip. Rate	0.878	0.902	0.812	0.912	0.749
LI	-0.974	-0.964	-0.971	-0.970	-0.932
Omega	0.301	0.772	-0.141	0.134	0.106
SFC Pressure	-0.816	-0.770	-0.809	-0.757	-0.699
Precip. Water	0.885	0.872	0.861	0.905	0.853
SFC RH	0.811	0.916	0.776	0.700	0.589
SFC Temperature	0.929	0.921	0.913	0.938	0.889
2m SHUM	0.926	0.920	0.908	0.939	0.887
10m U Wind	-0.170	-0.353	0.201	-0.100	0.080
10m V Wind	0.902	0.932	0.904	0.860	0.845

IV. DISCUSSION AND PRELIMINARY CONCLUSIONS

ENSO related inter-annual lightning variability occurs over much of the tropics and subtropics, with different mechanisms at play for each location. Several areas identified here agree with the previous findings including Argentina, Brazil, Australia, the Gulf of Mexico, and Equatorial Pacific and Atlantic. Potentially new findings are the regional ENSO teleconnections of the three African locations (including the one near the Red Sea and Djibouti) and the sensitivity of the Middle East.

In Africa, much of the variability can be explained with how ENSO phase interacts with the ITCZ, affecting both its location and strength. Warm phases favor a stronger ITCZ that remains north for longer. This may prolong and enhance lightning activity further north, into the Central Africa region. Cold phases favor a faster southerly surge of the ITCZ during the austral spring and summer, possibly promoting enhanced convective rainfall and lightning activity farther south. The annual variation in ITCZ position is possibly explained by the position of the Indian Ocean high (IOH). Under the enhanced easterly flow of La Niña, the IOH tends to push further westward during the austral summer, promoting the enhancement in northerly momentum. This inverse is true during El Niño, favoring a more easterly position of the IOH and enhanced southerly flow.

Cuba and the Florida Peninsula are not free of possible ENSO variability, however the impacts are not as straightforward. There is a potential signature from the increased southerly push of the polar jet during warm phases that is associated with the increase in severe weather potential throughout Florida but it occurs when the lightning activity is just beginning to increase and long before the lightning peak in the year, and is only observed in one of the warm phase years. There is also a possibility of a cancelling effect between the warm and cold phases where differences in stability shift the convective modes enough between them to promote fewer, stronger storms during the cooler and more stable warm phase and potentially more weak storms during the less stable La Niña.

More investigation is needed however to affirm these speculations as meaningful conclusions. Given the very limited number of ENSO phases to work with, there is a significant risk for bias towards outlier years that may not be entirely possible to account for without increasing the number of individual ENSO phases.

V. FUTURE WORK

As stated earlier in the paper, there are several ideas for expanding this study to increase both the depth and breadth. The most immediate is to finish the analysis of the other seven locations listed previously for environmental sensitivities to ENSO phase, and incorporate more model data beyond just the surface variables. Inclusion of OTD and the additional 3 years of data it collected before LIS was launched, including the 1997/1998 El Niño, is of significant interest. Comparing magnitudes of variables directly to the magnitudes of the lightning data to perform a regression analysis using the daily maximum values instead of daily averaged values is something currently being experimented with as well. Additionally, using conditional flash rates as outlined by Cecil et al., [2015] to determine the intensity of the storms occurring to further test the impacts of ENSO phase on storm intensity, such as in the Cuban and Central African regions. Ultimately, inclusion of the International Space Station (ISS) LIS and Geostationary Lightning Mapper (GLM) datasets as they become available would go a long way in building lightning climatology and give a greater number of ENSO phases to test against. Weighting each year in reference to the intensity could also yield some interesting results, as could dividing up the phases into more accurate classifications (e.g. warm to cold, cold to warm, cold to neutral, etc) but requires far more episodes than currently available.

ACKNOWLEDGMENTS

A.C. would like to thank Nathan Curtis and Alicia Carrubba for their help in editing and proofreading this paper.

LIS and OTD data, as used here, are distributed by the NASA EOSDIS Global Hydrology Resource Center DAAC, Huntsville, Alabama (http://lightning.nsstc.nasa.gov).

Any opinions, findings, and conclusions or recommendations expressed in this material are those of the author(s) and do not necessarily reflect the views of the National Aeronautics and Space Administration.

REFERENCES

Bolton, D., (1980), The computation of equivalent potential temperature. *Mon. Weather Rev*., 108, 1046–1053

Bovalo, C., C. Barthe, and N. Bègue, (2012), A lightning climatology of the south-west Indian Ocean. *Nat. Hazards Earth Syst. Sci.*, 12, 2659-2670, doi:10.5194/nhess-12-2659-2012

Cecil, D. J., D. Buechler, and R. Blakeslee, (2014), Gridded lightning climatology from TRMM-LIS and OTD: dataset description. *Atmos. Res.*, 135-136, 404–414, doi:10.1016/j.atmosres.2012.06.028 (data accessed from http://thunder.nsstc.nasa.gov on 7/15/2017)

Cecil, D. J., D. Buechler, and R. Blakeslee, (2015), TRMM LIS climatology of thunderstorm occurrence and conditional lightning flash rates. *J. Climate*, 28, 6536-6547, doi:10.1175/JCLI-D-15-0124.1

Christian, H. J. et al., (2003), Global frequency and distribution of lightning as observed from space by the Optical Transient Detector, *J. Geophys. Res.*, 108(D1), 4005, doi:10.1029/2002JD002347

Chronis, T. G. et al., (2008), Global lightning activity from the ENSO perspective, *Geophys. Res. Lett*., 35, L19804, doi:10.1029/2008GL034321

Collier, A. B. and A. R. W. Hughes, (2011), Lightning and the African ITCZ. *J. Atmos. Sol.-Terr. Phys.*, 73, 2392-2398, doi: 10.1016/j.jastp.2011.08.010

Dai, A. and T. M. L. Wigley, (2000), Global patterns of ENSO-induced precipitation. *Geophys. Res. Lett.*, 27, 9, 1283-1286, doi: 0094-8276/00/1999GL011140505.00

Dowdy, A. J., (2016), Seasonal forecasting of lightning and thunderstorm activity in tropical and temperate regions of the world, *Sci. Rep*., 6:20874, doi:10.1038/srep20874

Goodman, S. et al., (2000), The 1997-98 El Nino event and related wintertime lightning variations in the Southeastern United States, *Geophys. Res. Lett*., 27, 4, 541-544, doi:0094-8276/00/1999GL010808505.00

Hamid, E. Y., Z. Kawasaki, and R. Mardiana, (2001), Impact of the 1997–1998 El Niño event on lightning activity over Indonesia, *Geophys. Res. Lett*., 28, 147–150.

Huang, B. et al., (2017), Extended reconstructed sea surface temperature, version 5 (ERSSTv5): upgrades, validations, and intercomparisons, *J. Climate*, 30, 8179-8205, doi:10.1175/JCLI-D-16-0836.1 (data accessed from http://origin.cpc.ncep.noaa.gov/products/analysis_monitoring/ensostuff/ONI_v5.php on 8/4/17)

Jury, M. R., B. Pathack, and B. J. Sohn, (1992), Spatial structure and inter-annual variability of summer convection over southern Africa and the SW Indian Ocean, *S. Afr. J. Sci.*, 88, 275-280

Kalnay et al., (1996), The NCEP/NCAR 40-year reanalysis project, *Bull. Amer. Meteor. Soc.*, 77, 437-470 (data accessed from ftp://ftp.cdc.noaa.gov/Datasets/ncep.reanalysis.dailyavgs/ on 10/17/2017)

Koshak, B. et al., (2015), Variability of CONUS lightning in 2003-12 and associated impacts. *J. App. Meteor. Climatol.*, 54, 15-41, doi: 10.1175/JAMC-D-14-0072.1

Laing, A. et al., (2008), The influence of the El Nino-Southern Oscillation on cloud-to-ground lightning activity along the Gulf Coast. Part II: Monthly correlations. *Mon. Wea. Rev*., 136**,** 2544–2556, doi: 10.1175/2007MWR2228.1

LaJoie M. and A. Laing, (2008), The influence of the El Nino-Southern Oscillation on cloud-to-ground lightning activity along the Gulf Coast. Part I: Lightning climatology. *Mon. Wea. Rev.*, 136, 2523-2542, doi: 10.1175/2007MWR2227.1

Latif, M. et al., (1998), A review of the predictability and prediction of ENSO. *J. Geophys. Res.* 103, 14375–14393, doi: 10.1029/97JC03413

Nassor, A. and M. R. Jury, (1997), Intra-Seasonal climate variability of Madagascar. Part 2: Evolution of flood events , *Meteor. Atmos. Phys.*, 64, 243-254

Riemann-Campe, K., K. Fraedrich, and F. Lunkeit, (2009), Global climatology of convective available potential energy (CAPE) and convective inhibition (CIN) in ERA-40 reanalysis, *Atmos. Res.*, 93, 534-545, doi:10.1016/j.atmosres.2008.09.037

Ropelewski, C. F. and M. S. Halpert, (1986), North American precipitation and temperature patterns associated with the El Niño/Southern Oscillation (ENSO). *Mon. Wea. Rev.*, 114, 2352-2362.

Ropelewski, C. F. and M. S. Halpert, (1987), Global and regional scale precipitation patterns associated with the El Niño/Southern Oscillation, *Mon. Wea. Rev*., 115, 1606-1626.

Sátori, G., E. Williams, and I. Lemperger, (2009), Variability of global lightning activity on the ENSO time scale, *Atmos. Res.*, 91, 500-507, doi:10.1016/j.atmosres.2008.06.014

Trenberth, K. E., (1997), The definition of El Niño. *Bull. Amer. Meteor. Soc.*, 78**,** 2771–2777

Wright, P. B. et al., (1998), Correlation structure of the El Niño/Southern Oscillation phenomenon. *J. Climate*, 1, 609-625